Liquid Crystals
Publication details, including instructions for authors and subscription information:
http://www.informaworld.com/smpp/title~content=t713926090

X-ray structures of dilaterally substituted racemic nematogens containing a chiral centre in one of the lateral chains

H. Allouchi; M. Cotrait; C. Canlet; J. -P. Bayle

To cite this Article Allouchi, H. , Cotrait, M. , Canlet, C. and Bayle, J. -P.(2001) 'X-ray structures of dilaterally substituted racemic nematogens containing a chiral centre in one of the lateral chains', Liquid Crystals, 28: 8, 1177 — 1183
To link to this Article: DOI: 10.1080/02678290110047896
URL: http://dx.doi.org/10.1080/02678290110047896

LIQUID CRYSTALS, 2001, VOL. 28, NO. 8, 1177–1183

X-ray structures of dilaterally substituted racemic nematogens containing a chiral centre in one of the lateral chains

H. ALLOUCHI
Laboratoire de Chimie Physique—PIMIR E. A. 2098,
Faculté des Sciences Pharmaceutiques, 31 avenue Monge, 37200 Tours, France

M. COTRAIT
Laboratoire de Chimie Organique et Organométallique, UMR 5802 CNRS,
351 Cours de la Libération, Université Bordeaux I, 33405 Talence Cedex, France

C. CANLET and J.-P. BAYLE*
Laboratoire de Chimie Structurale Organique, URA CNRS 1384,
Université Paris XI, Bât, 410. 91405 Orsay Cedex, France

(*Received 18 November 2000; accepted 18 January 2001*)

A bifurcated and an open chain (linear) can be introduced laterally into mesogens containing four rings in the main core. The racemic compounds give a narrow nematic range. The X-ray crystal structures of two isomeric compounds show that the bifurcated chain is not aligned along the core as the linear one is. This unfavourable arrangement may be the cause of the deleterious effect of the bifurcated chain on the nematic range.

1. Introduction

Various flexible lateral substituents can be grafted on an elongated core containing four rings without disturbing the liquid crystal properties [1–5]. For compounds containing two nearby lateral substituents on the same inner aromatic ring, we have shown that the occurrence of the mesophase is due to the folding of the flexible lateral substituent along the core. To assume this folding, a flexible initial OCH_2 fragment is advisable. This folding back preserves the molecular anisotropy needed for the packing in the mesophase. To avoid steric hindrance, it has been shown that two nearby lateral alkoxy chains will fold back in opposite directions, as depicted in figure 1 (*a*), maintaining the molecular anisotropy: this is the key to the liquid crystal phase's existence [6]. The C_{ring}–O–C–C first fragment within the chain adopts a *gauche* conformation to allow this folding, the far part of the chain being roughly in a classical all-*trans*-conformation.

Instead of two nearby lateral chains, the possibility of using one bifurcated chain has been successfully explored [7]. In these compounds, the two branches of the bifurcated chain are also expected to point in opposite directions as proposed in figure 1 (*b*). Compounds with a more complex bifurcated lateral fragment (alkyl and aromatic branches) have also been obtained in the racemic and the enriched forms [8]. All these compounds possess large liquid crystalline ranges. Thus, the problem addressed in this paper is rather simple: can we

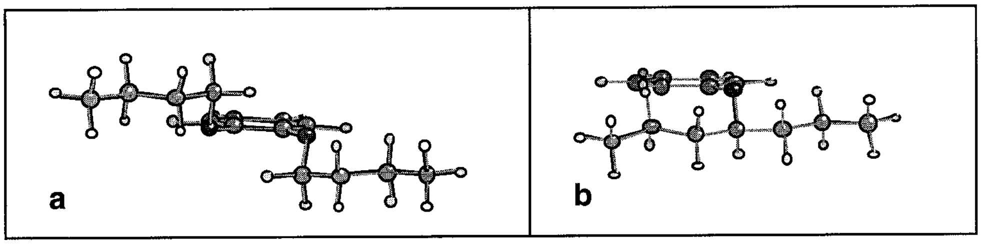

Figure 1. Idealized mean conformation of the chains substituted on the inner ring of the mesogen: (*a*) two alkoxy chains, (*b*) a single bifurcated chain.

---

*Author for correspondence; e-mail: jpbayle@icmo.u-psud.fr.

Liquid Crystals ISSN 0267-8292 print/ISSN 1366-5855 online © 2001 Taylor & Francis Ltd
http://www.tandf.co.uk/journals
DOI: 10.1080/02678290110047896

make the lateral substitution more complex and for example eventually obtain mesomorphic compounds having two bifurcated chains with good liquid crystalline properties?

The purpose of this is quite simple and involves obtaining mesogenic molecules containing the largest fraction of aliphatic motifs in lateral positions. If these aliphatic motifs contain the oxyethylene unit, these molecules will be able to dissolve salts and lead to conducting liquid crystals [9]. Therefore, in this paper, we want to present the first compounds containing a lateral linear hexyloxy chain and a nearby bifurcated alkyloxy chain. The X-ray crystal structures of the two compounds are presented in order to correlate the structure and the stability of the mesophase.

2. Results and discussion

2.1. *Synthesis*

We chose the simplest bifurcated alkyl fragment: 2-butyl. Thus, as an example, we describe in figure 2 the synthesis of 2-hexyloxy-3-(1-methylpropyloxy)-4-(4-chlorobenzoyloxy)-4′-(4-methylbenzoyloxy)azobenzene (labelled **3C***). **2C*** is the isomeric compound where the bifurcated chain and the linear one are interchanged. 2-Hexyloxy-3-(1-methylpropyloxy)phenol was prepared in two steps by selective etherification of 1,2,3-trihydroxybenzene [10]. *p*-Toluic acid was esterified with *p*-nitrophenol using the DCC method in dichloromethane [11]. The nitro group in this compound was selectively reduced using the $NiCl_2$/$NaBH_4$ reducing system [12]. After acidification, the crude solid amine hydrochloride, which had precipitated, was used for the diazotization step; this was performed at room temperature in PEG 200 as solvent, followed by coupling of the diazonium salt with the disubstituted phenol under basic conditions. The crude phenol was chromatographed using CH_2Cl_2 as eluent and was then esterified with 4-chlorobenzoyl chloride in $CHCl_3$/pyridine (50/50) as solvent. The final mesogen was chromatographed twice with CH_2Cl_2/hexane mixture (80/20) on silica gel (60–220 mesh).

2.2. *Transition temperatures*

The transition temperatures of the two compounds **2C*** and **3C*** are given in table 1 and compared with the compound having the same core, but carrying two linear pentyloxychains as lateral substituents (referred to as **diC5** [2]) and having 10 carbons in the lateral chains like **2C*** and **3C***. It is clear that the relative positioning of the bifurcated chain has no obvious influence on the transition temperatures, whereas the replacement of the linear chain in **diC5** by the bifurcated chain increases the melting temperature and strongly decreases the clearing temperature.

The mesophase is therefore less stable, whilst the increase in the melting temperature (average of + 25°C) must certainly be related to the increase in intermolecular interactions in the solid phase. These dipole–dipole interactions may result from the poor overlapping of the −COO− polar link with the bulky bifurcated chain when compared to the better overlapping of this link with the linear chain. The decrease in the clearing temperature (29°C) is related to the disorder in the nematic packing introduced by the methyl group belonging to the bifurcated chain. In the nematic phase, it has been shown that lateral chains are stacked along the core, their motions are reduced due to the packing of the molecules in the

Table 1. Transition temperatures of **2C*** and **3C***.

Compound	Cr	→	N	→	I
2C*	●	128[a]	●	131[a]	●
3C*	●	117	●	131	●
diC5	●	99.5	●	160	●

[a] Obtained by optical measurement.

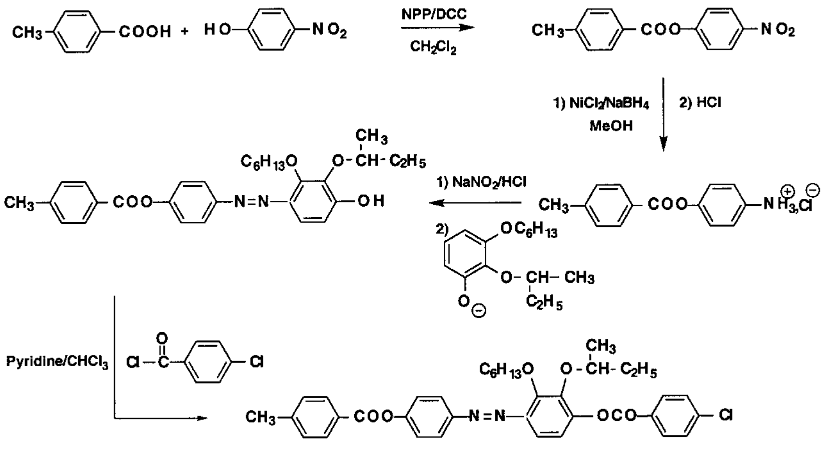

Figure 2. Synthetic scheme for compound **3C***.

nematic phase and there is little conformational disordering along the chain [2]. By adding a bifurcation within a chain, the methyl group broadens the molecule and increases the molecular separation, allowing a more pronounced disordering of all parts of the mesogens. This spacing factor obviously explains the decrease in the mesophase stability.

2.3. *Crystal structure determination and refinement*

Suitable crystals of **3C*** and **2C*** were grown from $CHCl_3$ solutions at 293 K. The crystal setting, the cell parameters and the data collection were performed with a CAD-4 Enraf–Nonius diffractometer, equipped with a graphite monochromator for the CuK_α radiation. The crystal data, data collection and refinement characteristics are given in table 2. Twenty-five reflections with q between 25° and 37° for **3C***, and 23° and 41° for **2C***, were used for the crystal setting and the least-squares refinement of cell parameters. The absorption correction was performed using the y-scan technique [13]. The crystal structures were solved by direct methods, using the MITHRIL package [14], which led to the positions of the core atoms and a few atoms at the beginning of the alkoxy lateral chains. The remaining atoms were located with great difficulty after successive Fourier syntheses. The atomic parameters were refined anisotropically with the SHELX93 package [15] for the non-hydrogen atoms (the hydrogen atoms were placed on their theoretical positions and allowed to ride with the carbon atoms to which they are attached) using constraints on the C–C bond lengths and C–C–C bond angles of the alkyl chains.

2.4. *Structure analysis*

The fractional atomic coordinates and the equivalent U_{eq} thermal motion factors are given in tables 3 and 4, respectively, for **3C*** and **2C***. The U_{eq} factors for the polyaromatic cores in both structures are quite low; those of the lateral alkoxy chains increase progressively from beginning to end. There are two possible conformations for the chiral chain of **2C***. The bond lengths are given in table 5 for **2C*** and **3C***. The X-ray structure and the atomic labelling are represented in figure 3 for **3C*** and figures 4 (*a*, *b*) for the two conformers of **2C***. Both chains, and particularly the hexyloxy chains, show a high thermal motion and are more or less disordered.

The four benzene rings are labelled as follow: ϕ1 (atoms C1 to C6), ϕ2 (atoms C10 to C15), ϕ3 (atoms C20 to C25) and ϕ4 (atoms C30 to C35). They are perfectly planar like the C–N=N–C group. The two

Table 2. Data collection and refinement characteristics for compounds **3C*** and **2C***.

Data collection	Compound **3C***	Compound **2C***
Chemical formula	$C_{37}H_{39}N_2O_6Cl$	$C_{37}H_{39}N_2O_6Cl$
Molecular mass/g mol^{-1}	643.2	643.2
Crystal system	monoclinic	triclinic
Space group	$P2_1/n$	$P\bar{1}$
Number of molecules per unit cell (Z)	4	2
a/Å	24.868(6)	10.829(7)
b/Å	5.485(3)	15.000(7)
c/Å	26.118(6)	11.718(5)
α/°	90.00	91.04(3)
β/°	82.71(2)	113.77(5)
γ/°	90.00	90.11(5)
Volume of cell/Å^3	3534	1742
Density/g cm^{-3}	1.209	1.227
Radiation	CuK_α	CuK_α
Absorption μ mm^{-1}	1.337	1.356
h_{min}, h_{max}	0; 27	0; 13
k_{min}, k_{max}	0; 6	− 18; 18
l_{min}, l_{max}	− 29; 29	− 14; 14
θ_{max}/°	60	60
Measured reflections	5231	6602
Observed reflections	1748	4345
Criteria	$I > 3s(I)$	$I > 3s(I)$
R_{int}/%	0.72	0.45
Refinement	on $F2$	on $F2$
Refined parameters	417	452
Weight	$1/[s^2(F_o^2) + (0.166P)^2 + 0.0000P]$	$1/[s^2(F_o^2) + (0.171P)^2 + 1.0374P]$
R	0.079	0.083
wR	0.094	0.107
S	1.31	1.03

Table 3. Fractional atomic coordinates and equivalent U_{eq} factors for the structure of **3C***.

Atom	x/a	y/b	z/c	$U_{eq}/\text{Å}^2$
C1	0.6959(4)	0.096(3)	0.6857(4)	0.161(4)
C2	0.6784(4)	0.266(2)	0.7190(4)	0.167(3)
C3	0.6270(3)	0.238(2)	0.7349(3)	0.145(3)
C4	0.5971(3)	0.039(2)	0.7156(3)	0.119(2)
C5	0.6162(3)	− 0.125(2)	0.6827(3)	0.149(3)
C6	0.6659(4)	− 0.098(2)	0.6682(4)	0.169(4)
C7	0.5418(4)	− 0.003(2)	0.7297(3)	0.122(3)
O8	0.5270(2)	0.174(1)	0.7613(2)	0.115(2)
O9	0.5132(2)	− 0.164(1)	0.7149(2)	0.168(2)
C10	0.4752(3)	0.150(1)	0.7788(3)	0.103(2)
C11	0.4328(3)	0.270(1)	0.7525(2)	0.108(2)
C12	0.3828(3)	0.249(1)	0.7682(2)	0.097(2)
C13	0.3761(2)	0.105(1)	0.8107(2)	0.090(2)
C14	0.4201(3)	− 0.008(1)	0.8383(2)	0.091(2)
C15	0.4714(3)	0.007(1)	0.8222(3)	0.095(2)
N16	0.3252(2)	0.063(1)	0.8297(2)	0.094(2)
N17	0.2887(2)	0.189(1)	0.8080(2)	0.102(2)
Cl18	0.76043(10)	0.154(1)	0.6672(1)	0.251(2)
C19	− 0.1437(3)	− 0.068(2)	0.9601(4)	0.207(4)
C20	0.2370(3)	0.145(1)	0.8260(2)	0.090(2)
C21	0.1963(3)	0.303(1)	0.8097(2)	0.111(2)
C22	0.1458(3)	0.281(1)	0.8254(3)	0.116(2)
C23	0.1371(3)	0.092(1)	0.8567(2)	0.093(2)
C24	0.1756(3)	− 0.070(1)	0.8736(2)	0.111(2)
C25	0.2256(3)	− 0.045(1)	0.8581(3)	0.111(2)
O26	0.0856(2)	0.048(1)	0.8715(2)	0.111(2)
C27	0.0647(3)	0.208(2)	0.9019(3)	0.111(2)
O28	0.0878(2)	0.390(1)	0.9175(2)	0.165(2)
C30	0.0105(3)	0.134(1)	0.9155(2)	0.102(2)
C31	− 0.0141(3)	0.283(1)	0.9480(3)	0.147(3)
C32	− 0.0632(4)	0.215(2)	0.9621(3)	0.148(3)
C33	− 0.0884(3)	0.011(2)	0.9439(3)	0.136(3)
C34	− 0.0641(4)	− 0.131(1)	0.9097(3)	0.154(3)
C35	− 0.0145(3)	− 0.070(1)	0.8962(3)	0.129(3)
O36	0.5143(2)	− 0.112(1)	0.8460(2)	0.116(2)
C37	0.5523(4)	0.037(2)	0.8803(4)	0.195(5)
C38	0.5996(7)	− 0.160(3)	0.884(1)	0.522(24)
C39	0.6422(9)	0.025(4)	0.888(1)	0.527(24)
C40	0.5371(5)	0.063(4)	0.9345(6)	0.330(10)
O41	0.4151(1)	− 0.130(1)	0.8832(2)	0.0996(12)
C42	0.4095(3)	− 0.379(1)	0.8775(3)	0.130(2)
C43	0.4003(3)	− 0.491(1)	0.9279(3)	0.149(3)
C44	0.3453(6)	− 0.432(2)	0.9418(5)	0.237(5)
C45	0.3175(6)	− 0.587(3)	0.9713(6)	0.272(6)
C46	0.2559(7)	− 0.570(4)	0.9763(9)	0.339(10)
C47	0.2545(8)	− 0.390(4)	1.013(1)	0.430(16)

Table 4. Fractional atomic coordinates and equivalent U_{eq} factors for the structure of **2C***.

Atom	x/a	y/b	z/c	$U_{eq}/\text{Å}^2$
C1	0.5490(4)	0.4322(3)	0.6720(4)	0.0734(9)
C2	0.6175(4)	0.4109(3)	0.5998(4)	0.0774(10)
C3	0.7082(4)	0.4716(2)	0.5883(4)	0.0705(9)
C4	0.7278(3)	0.5537(2)	0.6483(3)	0.0613(8)
C5	0.6534(4)	0.5750(3)	0.7176(4)	0.0784(10)
C6	0.5652(4)	0.5152(3)	0.7299(4)	0.0822(11)
C7	0.8231(3)	0.6210(2)	0.6419(3)	0.0658(8)
O8	0.8939(3)	0.5905(2)	0.5760(3)	0.0760(7)
O9	0.8402(3)	0.6940(2)	0.6877(3)	0.0967(10)
C10	0.9976(4)	0.6463(2)	0.5743(4)	0.0672(8)
C11	0.9731(4)	0.6996(3)	0.4739(4)	0.0726(9)
C12	1.0791(4)	0.7466(2)	0.4672(3)	0.0679(8)
C13	1.2085(3)	0.7401(2)	0.5608(3)	0.0626(8)
C14	1.2307(3)	0.6892(2)	0.6646(3)	0.0642(8)
C15	1.1227(4)	0.6401(2)	0.6706(4)	0.0680(9)
N16	1.3255(3)	0.7781(2)	0.5526(3)	0.0681(7)
N17	1.2996(3)	0.8308(2)	0.4657(3)	0.0730(8)
Cl18	0.4385(1)	0.3552(1)	0.6882(1)	0.1043(5)
C19	2.1561(4)	1.1129(3)	0.1668(4)	0.0841(11)
C20	1.4148(3)	0.8618(2)	0.4480(3)	0.0666(8)
C21	1.3904(4)	0.9261(3)	0.3601(4)	0.0874(12)
C22	1.4922(4)	0.9585(3)	0.3310(5)	0.0901(12)
C23	1.6181(4)	0.9260(3)	0.3896(4)	0.0727(9)
C24	1.6466(4)	0.8622(3)	0.4794(4)	0.0766(10)
C25	1.5442(4)	0.8302(3)	0.5085(4)	0.0734(9)
O26	1.7212(3)	0.9645(2)	0.3625(3)	0.0841(8)
C27	1.7772(4)	0.9145(2)	0.2987(3)	0.0671(8)
O28	1.7458(3)	0.8385(2)	0.2690(3)	0.0942(9)
C30	1.8764(3)	0.9666(2)	0.2699(3)	0.0632(8)
C31	1.9333(4)	0.9279(2)	0.1949(3)	0.0708(9)
C32	2.0229(4)	0.9751(3)	0.1624(3)	0.0726(9)
C33	2.0576(4)	1.0622(2)	0.2026(3)	0.0685(9)
C34	2.0014(4)	1.1008(3)	0.2787(4)	0.0778(10)
C35	1.9117(4)	1.0537(3)	0.3128(4)	0.0732(9)
O36	1.3565(2)	0.6822(2)	0.7581(2)	0.0766(7)
C37	1.4040(20)	0.7612(15)	0.8351(15)	0.124(9)
C38	1.3350(14)	0.7786(11)	0.9254(12)	0.125(4)
C39	1.3803(25)	0.8724(12)	0.9942(18)	0.144(6)
C40	1.5581(11)	0.7629(15)	0.9026(17)	0.164(7)
C137	1.3814(20)	0.7340(15)	0.8728(13)	0.123(7)
C138	1.4168(23)	0.8239(11)	0.8584(17)	0.154(7)
C139	1.4373(49)	0.8924(15)	0.9551(23)	0.278(24)
C140	1.4865(22)	0.6793(13)	0.9681(11)	0.189(9)
O41	1.1391(3)	0.5887(2)	0.7700(3)	0.0792(7)
C42	1.1939(6)	0.5031(3)	0.7632(6)	0.111(2)
C43	1.1881(6)	0.4438(4)	0.8587(7)	0.125(2)
C44	1.0532(6)	0.4218(4)	0.8531(7)	0.122(2)
C45	1.0433(7)	0.3596(5)	0.9409(8)	0.152(3)
C46	0.9072(9)	0.3405(6)	0.9346(10)	0.181(4)
C47	0.8472(9)	0.2650(6)	0.8867(12)	0.260(8)

benzoate groups ϕ1–COO and OOC–ϕ4 are planar. The dihedral angles ϕ2/ϕ1COO, ϕ3/ϕ2 and OOCϕ4/ϕ3 are presented in table 4 for compounds **2C***, **3C*** and for compound **diC5** for comparison. The core conformations for the three molecules are very similar.

Significant torsional angles for **2C*** and **3C*** are presented in table 7. The hexyloxy chain in **2C*** and **3C*** is folded back along the core, as is the case for the homologuous compound **diC5**, for which the conformation is more or less all-*trans* [6]. The bifurcated chain does not have the conformation expected from figure 1(*b*). The methyl group strongly perturbs the folding of the bifurcated chain and this conformation may explain the difference in the melting and clearings temperatures of **2C***, **3C*** and **diC5**.

Table 5. Bond lengths (Å) for **3C*** and **2C***.

Bond	3C*	2C*	Bond	3C*	2C*
C1–C6	1.34(1)	1.383(6)	C22–C23	1.354(8)	1.352(6)
C1–C2	1.38(1)	1.365(5)	C23–C24	1.342(7)	1.376(6)
C1–Cl18	1.76(1)	1.728(4)	C23–O26	1.405(6)	1.404(4)
C2–C3	1.40(1)	1.386(5)	C24–C25	1.362(7)	1.373(5)
C3–C4	1.38(1)	1.380(5)	O26–C27	1.33(1)	1.355(5)
C4–C5	1.37(1)	1.360(5)	C27–O28	1.20(1)	1.193(4)
C4–C7	1.49(1)	1.466(5)	C27–C30	1.49(1)	1.476(5)
C5–C6	1.35(1)	1.360(5)	C30–C35	1.35(1)	1.386(5)
C7–O9	1.17(1)	1.191(4)	C30–C31	1.38(1)	1.382(5)
C7–O8	1.35(1)	1.364(4)	C31–C32	1.37(1)	1.376(5)
O8–C10	1.426(7)	1.406(4)	C32–C33	1.34(1)	1.381(5)
C10–C11	1.350(7)	1.371(5)	C33–C34	1.38(1)	1.386(6)
C10–C15	1.393(8)	1.375(5)	C33–C34	1.38(1)	1.386(6)
C11–C12	1.364(8)	1.374(5)	C34–C35	1.37(1)	1.385(6)
C12–C13	1.389(7)	1.394(5)	O36–C37	1.47(1)	1.44(1)
C13–C14	1.378(7)	1.385(5)	C37–C40	1.52(1)	1.53(1)
C13–N16	1.436(7)	1.427(5)	C37–C38	1.59(2)	1.54(1)
C14–O41	1.370(6)		C38–C39	1.46(2)	1.56(1)
C14–O36		1.368(4)	O41–C42	1.377(6)	1.430(5)
C14–C15	1.396(8)	1.407(5)	C42–C43	1.50(1)	1.463(7)
C15–O36	1.335(6)		C43–C44	1.49(1)	1.472(8)
C15–O41		1.361(4)	C44–C45	1.39(1)	1.436(8)
N16–N17	1.220(5)	1.241(4)	C45–C46	1.56(1)	1.473(9)
N17–C20	1.443(7)	1.423(4)	C46–C47	1.38(2)	1.37(2)
C19–C33	1.551(9)	1.503(4)	O36–C137		1.47(1)
C20–C21	1.359(7)	1.371(5)	C137–C138		1.43(3)
C20–C25	1.390(8)	1.380(5)	C137–C140		1.49(3)
C21–C22	1.377(8)	1.369(6)	C138–C139		1.46(3)

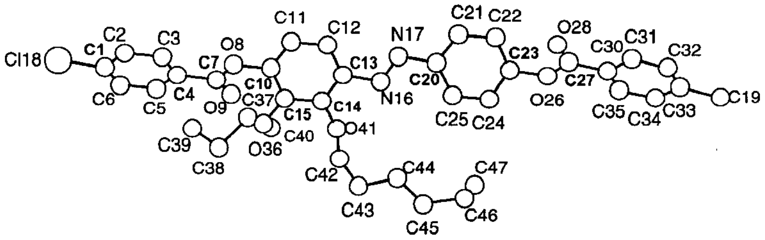

Figure 3. X-ray structure and atomic labelling for compound **3C***.

Table 6. Dihedral angles between mean planes of contiguous rings in compounds **diC5**, **3C*** and **2C***.

Angle (°)	**diC5**	3C*	2C*
$\phi 2/\phi 1$	82.5	86.2	84.9
$\phi 3/\phi 2$	31.4	17.9	23.7
$\phi 4/\phi 3$	76.0	67.2	72.3

The projections of the structures on the (*xOz*) plane are given in figures 5 and 6. The molecular axes are strictly parallel for **3C*** and quasi-parallel for **2C***, arrangements that are very typical for nematogenic structures.

It is noted that in the structure of compound **3C***, the molecules are associated in pairs, through dipole–dipole interactions between the COO groups of two contiguous molecules: this involves the parent molecule (x, y, z) and its partner $(1/2 - x, 1/2 + y, 3/2 - z)$, through the 21 axis with:

$$d[\mathrm{O26}(x, y, z) \ldots \mathrm{O9}(1/2 - x, 1/2 + y, 3/2 - z)] = 3.49\ \text{Å}$$

$$d[\mathrm{O28}(x, y, z) \ldots \mathrm{O9}(1/2 - x, 1/2 + y, 3/2 - z)] = 4.02\ \text{Å}.$$

This kind of association is very common in the structures of smectogenic compounds and corresponds to mode I, according to Hori *et al.* [16]. These pairs interact with the contiguous pairs through numerous weak van der Waals interactions.

3. Conclusion

We have synthesized the first two mesogenic molecules containing four aromatic rings in the core and two lateral substituents in one of the inner rings, these being

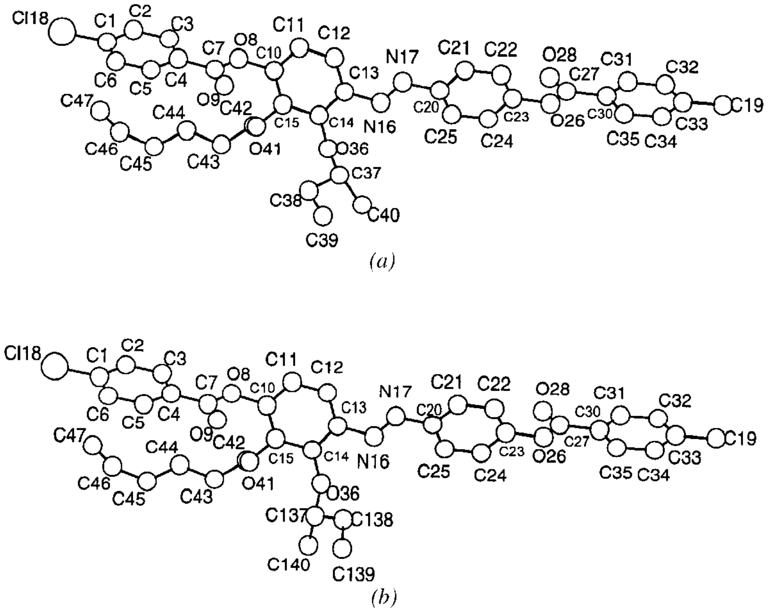

Figure 4. X-ray structure and atomic labelling for (*a*) compound **2C*a**, (*b*) compound **2C*b**.

Table 7. Significant torsion angles[a] (°) for compounds **2C*** and **3C***.

Torsion angle	3C*	2C*
C5–C4–C7–C8	*trans*	*trans*
C4–C7–O8–C10	*trans*	*trans*
C7–O8–C10–C11	- 95.5(7)	- 98.2(3)
C22–C23–O26–C27	- 66.8(7)	- 111.3(4)
C23–O26–C27–C30	*trans*	*trans*
O26–C27–C30–C31	*trans*	*trans*
C13–C14–O36–C37		71.2(6)
C13–C14–O41–C42	98.4(7)	
C14–O36–C37–C38		74.6(9)
O36–C37–C38–C39		*trans*
C14–C15–O41–C42		- 82.2(4)
C14–C15–O36–C37	- 102.3(8)	
C15–O41–C42–C43		- 170.5(4)
C15–O36–C37–C38	- 164.4(13)	
O36–C37–C38–C39	147.1(18)	
O41–C42–C43–C44	71.1(10)	63.8(7)
C42–C43–C44–C45	150.6(13)	*trans*
C43–C44–C45–C46	- 164.3(13)	*trans*
C44–C45–C46–C47	- 81.7(25)	99.0(10)
C13–C14–O36–C137		106.7(7)
C14–O36–C137–C138		- 84.6(11)
O36–C137–C138–C139		*trans*

[a] Angles that differ by less than 10° from the trans-conformation (180°) are labelled 'trans'.

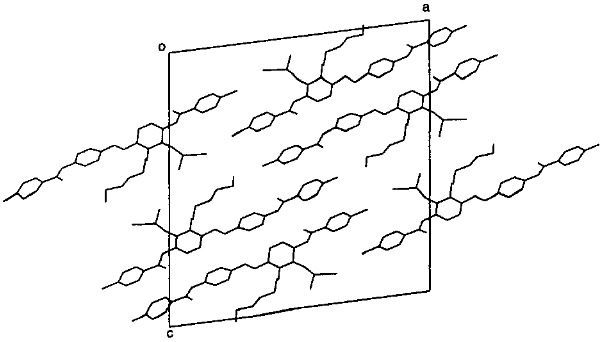

Figure 5. Projection of the structure on the (*xOz*) plane for compound **3C***.

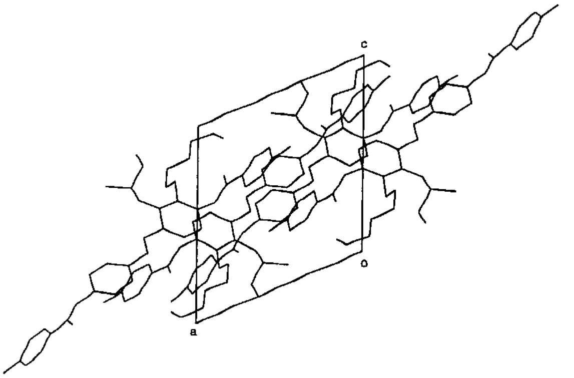

Figure 6. Projection of the structure on the (*xOz*) plane for compound **2C***.

a lateral hexyloxy chain positioned next to a bifurcated iso-butyloxy chain. The effect of this type of substitution compared with that involving a *n*-alkoxy group is deleterious to the mesogenic properties. The compounds are weakly enantiotropic nematogens. The two X-ray crystal structures are presented and it is shown that the decrease in the stability of the mesophase can be related to the unfavourable conformation of the bifurcated chain. This effect may be counterbalanced with longer bifurcated chains. Such a study is under progress and will be published separately.

References

[1] Perez, F., Judeinstein, P., Bayle, J.-P., Allouchi, H., Cotrait, M., and Lafontaine, E., 1996, *Liq. Cryst.*, **21,** 855.

[2] Perez, F., Bayle, J.-P., and Fung, B. M., 1996, *New. J. Chem.*, **20,** 537.

[3] Perez, F., Judeinstein, P., Bayle, J.-P., Roussel, F., and Fung, B. M., 1997, *Liq. Cryst.*, **22,** 711.

[4] Perez, F., Judeinstein, P., Bayle, J.-P., Allouchi, H., Cotrait, M., Roussel, F., and Fung, B. M., 1998, *Liq. Cryst.*, **24,** 627

[5] Canlet, C., Fung, B. M., Roussel, F., Leblanc, K., Berdaguè, P., and Bayle, J.-P., 2000, *Liq. Cryst.*, **27,** 635.

[6] Allouchi, H., Belaaraj, A., Cotrait, M., Lafontaine, E., Judeinstein, P., and Bayle, J.-P., 2000, *Liq. Cryst.*, **27,** 1087.

[7] Canlet, C., Judeinstein, P., Bayle, J.-P., Roussel, F., and Fung, B. M., 1998, *New J. Chem.*, 211.

[8] Canlet, C., Berdaguè, P., Judeinstein, P., and Bayle, J.-P., 1999, *Mol. Cryst. liq. Cryst.*, **332,** 207.

[9] Leblanc, K., Berdaguè, P., Rault, J., Bayle, J.-P., and Judeinstein, P., 2000, *Chem. Commun.*, 1291.

[10] Berdaguè, P., Perez, F., Courtieu, J., and Bayle, J.-P., 1993, *Bull. Soc. chim. Fr.*, **130,** 475.

[11] Hassner, A., and Alexanian, V., 1978, *Tetrahedron Lett.*, **46,** 4475.

[12] Nose, A., and Kudo, T., 1981, *Chem. Phar. Bull.*, **29,** 1159.

[13] North, A. C. T., Phillips, D. C., and Matthews, F. S., 1968, *Acta Cryst.*, **A24,** 351.

[14] Gilmore, C. J., 1984, *J. appl. Crystallogr.*, **17,** 42.

[15] Sheldrick, G. M., 1993, Program for the refinement of crystal structures. University of Gottingen, Germany.

[16] Hori, K., and Ohashi, Y., 1991, *Mol. Cryst. liq. Cryst.*, **203,** 371.